

JAST (Journal of Animal Science and Technology) TITLE PAGE
Upload this completed form to website with submission

ARTICLE INFORMATION	Fill in information in each box below
Article Type	Research article
Article Title (within 20 words without abbreviations)	Development of an oscillating magnetic field-assisted supercooling system for bovine embryo preservation
Running Title (within 10 words)	Hanwoo embryo supercooling preservation with a magnetic field
Author	Jun Hwi So ^{1#} , Byung Hyun Ju ^{2,3#} , Sung Yong Joe ⁴ , Youngbok Ko ^{5,6} , Soojin Jun ⁷ , Min Kyu Kim ^{2,3#} , Seung Hyun Lee ^{1, 4,6#} # These authors contributed equally to this work.
Affiliation	¹ Department of Smart Agriculture Systems, Chungnam National University, Daejeon 34134, Korea ² Division of Animal and Dairy Science, Chungnam National University, Daejeon 34134, Korea ³ MK Biotech Inc., Daejeon 34134, Korea ⁴ Department of Smart Agriculture Systems Machinery Engineering, Chungnam National University, Daejeon 34134, Korea ⁵ Department of Obstetrics and Gynecology, Chungnam National University, Daejeon 35015, Korea ⁶ Neo Vitalink Inc., Daejeon 34134, Korea ⁷ Department of Human Nutrition, Food, and Animal Sciences, University of Hawaii, Honolulu, HI 96822, USA
ORCID (for more information, please visit https://orcid.org)	Jun Hwi So (https://orcid.org/0000-0001-9479-6000) Byung Hyun Ju (https://orcid.org/0000-0003-1672-4604) Sung Yong Joe (https://orcid.org/0000-0002-8482-9777) Youngbok Ko (https://orcid.org/0000-0002-8972-6742) Soojin Jun (https://orcid.org/0000-0002-0865-4565) Min Kyu Kim (https://orcid.org/0000-0002-9259-8219) Seung Hyun Lee (https://orcid.org/0000-0002-2096-3053)
Competing interests	No potential conflict of interest relevant to this article was reported.
Funding sources State funding sources (grants, funding sources, equipment, and supplies). Include name and number of grant if available.	This research was funded by Chungnam National University, grant number 2024-0899-01.
Acknowledgements	Not applicable
Availability of data and material	Upon reasonable request, the datasets of this study are available from the corresponding author.
Authors' contributions Please specify the authors' role using this form.	Conceptualization: Kim MK, Lee SH Data curation: So JH, Ju BH, Kim MK, Lee SH Formal analysis: So JH, Ju BH, Ko YB Methodology: So JH, Ju BH, Joe SY, Jun SJ Software: So JH, Ju BH Validation: So JH, Ju BH Investigation: So JH, Ju BH Writing - original draft: So JH, Ju BH Writing - review & editing: So JH, Ju BH, Joe SY, Ko YB, Jun SJ, Kim MK, Lee SH
Ethics approval and consent to participate	The use of bovine ovaries in this study was reviewed and approved by the Institutional Animal Care and Use Committee of Chungnam National University (IACUC Approval No. 202103A-CNU-002).

CORRESPONDING AUTHOR CONTACT INFORMATION

For the corresponding author (responsible for correspondence, proofreading, and reprints)	Fill in information in each box below
First name, middle initial, last name	Seung Hyun Lee Min Kyu Kim
Email address - this is where your proofs will be sent	seungle2@cnu.ac.kr kminkyu@cnu.ac.kr
Secondary Email address	
Address	Department of Smart Agriculture Systems Machinery Engineering, College of Agriculture and Life Science, Chungnam National University, 99 Daehak-Ro, Yuseong-Gu, Daejeon, 34134, Republic of Korea Division of Animal and Dairy Science, Chungnam National University, Daejeon 34134, Korea
Cell phone number	+82-10-2519-9702
Office phone number	+82-42-821-6718
Fax number	+82-42-823-6246

ACCEPTED

Abstract

In-vitro-produced embryos have become an important biomaterial for accelerating genetic improvements in livestock, increasing the need for reliable short- and mid-term preservation strategies. This study was conducted to investigate the effects of oscillating-magnetic-field-assisted supercooling on the survival of bovine *in vitro* fertilization (IVF) embryos. A supercooling preservation system combining Helmholtz-type coils with a precise circulating cooling chamber was designed and fabricated to maintain the embryos in a uniform supercooled state. Blastocyst-stage embryos were preserved at -4°C in a hypothermic preservation medium under exposure to an OMF of 10 Hz with flux densities ranging from 0 to 20 mT.

The preservation medium remained stably supercooled at -4°C without freezing under all magnetic field conditions, and the magnetic flux density did not alter the cooling behavior. The embryos were preserved for 24 h and subsequently cultured for an additional 24 h to assess their post-preservation viability. Survival rates were higher in all magnetic field groups than in the control group (0 mT), with values of 48.66% (0 mT), 60.07% (5 mT), 62.85% (10 mT), 75.69% (15 mT), and 68.96% (20 mT). Notably, the 15 mT group exhibited the highest survival rate, showing a significant improvement over the control.

Although the magnetic field did not affect the supercooling characteristics of the preservation solution, it markedly enhanced embryo survival at -4°C . The results demonstrated that the application of an oscillating magnetic field did not disrupt the stability of the supercooled state while also improving cellular tolerance to low-temperature stress. These findings provide a promising foundation on which to develop magnetic-field-based non-freezing preservation technologies for biological specimens.

Keywords: Embryo, supercooling, oscillating magnetic field, temperature control, viability

22

23 **Introduction**

24 Embryos constitute the earliest stage of life and mark the onset of the reproductive process. Since the technological
25 advancements in *in vitro* fertilization (IVF) during the 1990s, the reliable *in vitro* production of high-quality embryos
26 has become feasible [1]. As a result, embryos have gained increasing importance as a biological resource for enhancing
27 genetic dissemination and reproductive efficiency. In this context, embryo preservation has progressed beyond simple
28 storage toward more advanced strategies aimed at maintaining viability for extended periods, thereby underscoring
29 the growing need for stable preservation and management systems, particularly in livestock production [2].

30 Embryo preservation methods are generally classified according to the storage duration into hypothermic
31 preservation (2-8 °C) for short-term storage and cryopreservation (-196 °C) for long-term storage. Slow freezing and
32 vitrification are widely used in cryopreservation and allow cells to be stored for long periods or even virtually
33 indefinitely. However, a major limitation of cryopreservation is the cellular damage caused by osmotic imbalances
34 and the formation of ice crystals during the freezing process [3]. Although vitrification has demonstrated improved
35 preservation outcomes in recent studies, it still requires high concentrations of cryoprotectants and considerable
36 technical expertise, making it unsuitable for short- and medium-term preservation [3,4]. On the other hand,
37 hypothermic preservation requires only simple equipment and handling procedures to extend the lifespan by
38 suppressing cellular metabolic activity. However, this method is inherently limited to very short-term preservation, as
39 survival declines rapidly due to membrane damage, ionic imbalances, and the accumulation of reactive oxygen species
40 [5]. To overcome these limitations, the substantial efforts have focused on alternative strategies, including
41 optimization of the cryoprotectant composition [6,7], controlled ice nucleation [8], high-pressure freezing [9], and
42 supercooling [10].

43 Among these preservation technologies, supercooling, capable of maintaining liquid products below their freezing
44 points without the formation of ice crystals, has been proposed as non-freezing preservation method that minimizes
45 cryoinjuries in cells and tissues [11,12]. However, because the supercooled state is thermodynamically metastable,
46 even minor perturbations such as mechanical vibrations, impurities, interfacial heterogeneities, or irregularities on
47 container surfaces can readily induce ice nucleation [13]. Therefore, precise control of the physical conditions is
48 essential to maintain a stable supercooled state.

49 Recent studies have explored the use of magnetic fields to suppress ice nucleation and stabilize the supercooled
50 state [14]. Previous studies indicated that magnetic fields can modulate the orientation of water molecules and the
51 organization of hydrogen-bond networks, thereby lowering the freezing onset temperature and slowing ice-crystal
52 growth [15]. In particular, oscillating magnetic fields (OMF), in which the magnetic polarity periodically reverses,
53 have been shown to inhibit ice crystallization within agricultural and biological materials [16,17]. Magnetic-field-
54 assisted supercooling preservation has been investigated primarily in relation to agricultural products, whereas studies
55 involving embryos are still extremely limited.

56 The objective of the present study was to develop an oscillating-magnetic-field (OMF)-assisted supercooling
57 preservation system based on the aforementioned physical principles. The system consists of a temperature-controlled
58 chamber integrated with a magnetic field generator to maintain embryos under stable thermal conditions while
59 applying periodic magnetic field oscillations. To verify system the performance capabilities, we evaluated the
60 supercooling stability and operational characteristics and assessed embryo survival after preservation at -4 °C under

61 magnetic flux densities of 0–20 mT as a biological validation metric. Through these evaluations, this study
62 demonstrates the feasibility of a magnetic-field-based supercooling platform for short- and medium-term embryo
63 preservation.

64 65 **Materials and Methods**

66 **Ethics**

67 The use of bovine ovaries in this study was reviewed and approved by the Institutional Animal Care and Use
68 Committee of Chungnam National University (IACUC Approval No. 202103A-CNU-002).

70 **Sample Preparation**

71 Bovine embryos were supplied by MK Biotech (Daejeon, Korea) using an IVF protocol. The embryos used in this
72 study were produced as described in a previous study [18] and were all at the blastocyst stage. Only morphologically
73 normal embryos that met the quality criteria were selected for the experiment. Within each independent experimental
74 run, embryos derived from multiple donor cows (3–6 donors per batch) were pooled prior to random allocation such
75 that embryos from each donor were distributed across all treatment groups, minimizing donor-specific bias.

76 The preservation solution used for the supercooling experiments was formulated by MK Biotech based on the
77 composition described in earlier work [6], which employed a tissue culture medium 199 (TCM 199; Gibco, Grand
78 Island, NE, USA) supplemented with fetal bovine serum (FBS; Gibco) and HEPES (Sigma-Aldrich Chemical, St.
79 Louis, MO, USA). Each embryo was individually placed in a 1.2 mL tube containing the preservation solution, with
80 6–9 embryos per group. Samples were transported in insulated containers with ice packs and were used for the
81 experiments immediately upon arrival.

82 83 **Experimental System Configuration**

84 The overall configuration of the supercooling and OMF system used in this study is shown in Fig. 1 (A). The system
85 consisted of a custom-built Helmholtz coil, a cooling chamber for embryo preservation, a circulating chiller (LC-
86 LT412, LKLAB Korea, Namyangju, Korea), and a custom-built programmable pulse power supply. The power supply
87 was designed to generate an alternating pulsed waveform with adjustable voltages (from 1 V to 200 V), on/off duty
88 cycles (from 10% to 90%), and frequencies (from 1 Hz to 20 kHz). The voltage and current applied to the Helmholtz
89 coil were continuously monitored and recorded in real time using a differential probe (PR-60, BK Precision, USA), a
90 current monitor (Model 150, Pearson Electronics, Palo Alto, CA, USA) and an oscilloscope (TBS1102B, Tektronix,
91 Beaverton, OR, USA). In this study, bipolar square-pulse voltage with a 50% duty cycle and 10 Hz frequency was
92 applied to the coils to generate the OMF.

93 As shown in Figure 1B, the Helmholtz coil pair was symmetrically positioned within the cooling chamber to
94 generate a uniform magnetic field throughout the chamber interior. The coil bobbins were spaced apart from the
95 chamber wall to minimize thermal and mechanical interference, and coil heating was controlled using surface heat
96 sinks combined with forced-air cooling fans (Fig. 1C). All experiments were conducted under laboratory ambient

97 conditions (≤ 25 °C), and a PID control system was employed to maintain the internal chamber temperature
98 independent of ambient temperatures or heat generation by the coil.

99 **(Fig. 1)**

100 **101 Cooling Chamber Design**

102 The cooling system was designed and manufactured to maintain a uniform temperature inside the chamber and to
103 withstand the thermal load associated with coolant circulation (Fig. 2 (A)). The main body of the chamber consisted
104 of a high-strength acrylic material with excellent thermal insulation properties and incorporated a double-wall
105 structure for enhanced stability. The samples were mounted on a three-tier rack installed inside the chamber, with four
106 sample tubes placed on each level, allowing a total of twelve samples to be accommodated simultaneously.

107 A propylene-glycol-based coolant (Antifreeze -60°F, Star Brite, FL, USA) was circulated within the system, with
108 the coolant flow rate set to 3 L/min. The inlet and outlet were positioned at the upper and lower sections of the chamber,
109 respectively, to establish a stable convective flow. The chamber opening was sealed with an acrylic cover and
110 polyethylene foam insulation to minimize heat loss. The chamber temperature was maintained at -4 °C ± 0.2 °C.

111 **(Fig. 2)**

112

113 **Helmholtz Coil Assembly**

114 A Helmholtz configuration, consisting of two identical circular coils positioned at a fixed distance, was adopted to
115 generate a uniform magnetic field (Fig. 3A). The magnetic flux density distribution was analyzed using COMSOL
116 Multiphysics v.6.2 (COMSOL AB, Stockholm, Sweden) based on a direct current (DC) magnetic field model for
117 simplicity and to approximate quasi-static field conditions, as described in a previous study [19]. The coils were wound
118 with copper wire with a diameter of 1 mm, comprising 490 turns per coil. Non-magnetic materials such as air, plastic,
119 the coolant, and the biological samples were neglected in the magnetic simulation (Fig. 3B).

120 The simulation results were used to evaluate the magnetic field distribution and to determine the optimal sample
121 placement region. After defining the placement positions, alternating voltage was applied to the coils, with the input
122 voltage adjusted to achieve a magnetic flux density of 15 mT at the designated sample locations.

123 **(Fig. 3)**

124

125 **Temperature Profile Measurements**

126 The internal temperature of the cooling chamber was measured and recorded in all experiments. All temperatures
127 were measured using T-type thermocouple (TT-T-36-SLE, Omega Engineering, Stamford, CT, USA) that minimizes
128 magnetization effects in the magnetic field environment. The T-type thermocouple, composed of non-magnetic Cu-
129 Constantan materials, is also known to exhibit minimal interference under magnetic fields [20]. For the solution-level
130 supercooling experiments, the thermocouple was attached to the outer surface of the sample tube. For the embryo
131 preservation experiments, the thermocouple was attached to the sample holder and positioned at the geometric center
132 of the cooling chamber to monitor the chamber air temperature. The thermocouples were connected to a data
133 acquisition unit (34970A, Keysight Technologies, Santa Rosa, CA, USA) to record temperature data at 5s intervals.

134

135 **Measurement of Supercooling Characteristics in Solutions**

136 The effects of the OMFs on the cooling behavior of the embryo preservation solution were analyzed in this study.
137 Each sample (1.2 mL) was placed inside the cooling chamber, and the magnetic field was applied when the
138 temperature inside cooling chamber reached -4°C . A preservation temperature of -4°C was selected based on
139 experimental design considerations and consistency with commonly adopted conditions in supercooling-based embryo
140 preservation studies. This temperature was chosen to enable stable maintenance of the supercooled state during short-
141 term preservation while remaining compatible with embryo viability. The magnetic field strength levels were set to 0
142 (control), 5, 10, and 15 mT. OMFs with a fixed frequency of 10 Hz were applied to all experimental groups. During
143 the cooling process, the temperature was continuously recorded in real time until the solution temperature stabilized
144 at -4°C .

145 Each sample consisted of 1.2 mL of preservation solution contained in a cell storage tube, and each was introduced
146 into the cooling chamber to analyze temporal variations in the temperature. Three samples were used per magnetic
147 field condition, and all experiments were repeated three times to ensure reproducibility. After reaching -4°C , the
148 samples were maintained at this temperature for 30 min. Successful maintenance of the supercooled state was defined
149 by the absence of visible ice formation and abrupt temperature increases indicative of latent heat release associated
150 with ice nucleation.

151

152 **Embryo Supercooling Preservation Procedure**

153 Embryo supercooling preservation experiments were conducted to evaluate the effects of the supercooled state on
154 embryo survival (Fig. 4). All experiments were performed in the cooling chamber maintained at -4°C , with magnetic
155 flux densities of 0 mT (control), 5 mT, 10 mT, 15 mT, and 20 mT applied. Solution-level experiments were limited to
156 magnetic flux densities in a range of 0–15 mT based on preliminary design considerations indicating that this range
157 was sufficient to evaluate solution-level supercooling stability, whereas the embryo preservation experiments included
158 20 mT to assess system performance at the upper operational limit of the magnetic field generator. Prior to sample
159 loading, the cooling system and magnetic field generator were pre-activated to ensure thermal and magnetic
160 stabilization inside the chamber.

161 After stabilization, the embryo samples were introduced into the chamber and preserved at -4°C for 23 hours.
162 Subsequently, the chamber temperature was gradually increased to 4°C over a one-hour rewarming step. The total
163 preservation time was 24 hours, after which all samples were immediately transferred to a modified CR2 medium
164 containing 5% FBS and incubated at 38.5°C under 5% CO_2 for 24 hours, based on culture conditions described
165 previously [18].

166 **(Fig. 4)**

167

168 **Viability Assessment of Preserved Embryos**

169 After the 24-hour preservation process, the embryos were transferred to an incubator and cultured for an additional
170 24 hours. The viability of each embryo was evaluated under a stereomicroscope based on morphological integrity.
171 The survival rate was calculated as follows:

172
$$\text{Survival rate}(\%) = \left(\frac{\text{Number of viable embryos}}{\text{Total number of embryos}} \right) \times 100$$

173

174 **Statistical Analysis**

175 All experiments were independently repeated at least three times. Statistical analyses were conducted using SPSS
176 Statistics v.19.0 (IBM, NY, USA). The mean survival rate from each independent trial was used to analyze differences
177 among groups. Data normality and homogeneity of variance were verified using the Shapiro-Wilk test and Levene's
178 test, respectively. One-way analysis of variance (ANOVA) was conducted, and Bonferroni correction was applied for
179 multiple comparisons when significant differences were detected. Differences were considered statistically significant
180 at $p < 0.05$.

181 **Results**

182 **System Performance Validation**

183 ***Temperature uniformity in the cooling chamber***

184 The temperature uniformity inside the cooling chamber was secured to ensure a stable cooling environment during
185 embryo preservation. As shown in Fig. 5, the temperature was recorded along both the vertical and horizontal
186 directions. For the vertical measurement, sample tubes were placed at three levels (upper, middle, and lower), while
187 for the horizontal measurement, four points were arranged in a circular pattern on the same level to evaluate any
188 temperature variations.

189 As summarized in Table 1, the reported temperature values represent deviations from the target chamber
190 temperature of -4°C . The average temperature deviations of the upper and lower levels were within $\pm 0.05^{\circ}\text{C}$ relative
191 to the middle level, with maximum deviations of 0.14°C at the top and 0.02°C at the bottom. Within each level, the
192 average temperature difference among the four measurement points was less than 0.015°C , with maximum deviation
193 of 0.1°C . Overall, the cooling chamber maintained a stable thermal environment centered at -4°C , with vertical and
194 horizontal temperature uniformity within $\pm 0.5^{\circ}\text{C}$ and $\pm 0.2^{\circ}\text{C}$, respectively.

195 **(Fig. 5)**

196 **(Table 1)**

197

198 ***Magnetic flux distribution of the Helmholtz coils***

199 The magnetic coils served as a key component for generating a uniform magnetic field within the embryo
200 preservation chamber. The magnetic flux distribution of the fabricated Helmholtz coils was validated through both
201 simulation and experimental measurements (Fig. 6). As shown in Fig. 6A, the designed Helmholtz configuration
202 produced a typical magnetic field-line pattern characteristic of this geometry. The coils generated an axial magnetic
203 field whose strength and direction were linearly proportional to the magnitude and polarity of the applied current.

When square-pulsed alternating current was applied to the coils, the magnetic field direction was periodically reversed, forming an oscillating magnetic field (OMF), as confirmed by experimental measurements (Fig. 6B). Under experimental operating conditions, stable OMF generation was achievable up to a magnetic flux density of 20 mT (data not shown). At higher magnetic field strength settings, heat generated in the coils could not be sufficiently dissipated, preventing stable operation. Based on magnetic field simulations, a uniform magnetic field region corresponding to $\pm 5\%$ of the target magnetic flux density (15 mT) was identified along the central axis of the coil ($y = 0$ mm) (Fig. 6C). This uniform region comprised three axial segments (-63 to -49 mm, -32 to -9 mm, and 9 to 32 mm). Accordingly, the sample positions were set to -60, -20, and +20 mm, each of which falls within one of the identified uniform-field segments.

While the simulation predicted a magnetic flux density of 15 mT at 3.1 A, the experimental measurement confirmed that 15 mT was achieved at a 3.2 A peak under alternating current excitation (Fig. 6D).

(Fig. 6)

Effects of the Magnetic Field on the Cooling Characteristics of the Solutions

The effects of different oscillating magnetic fields (OMFs) on the cooling behavior of the preservation solution were analyzed (Fig. 7). A differential scanning calorimetry (DSC) analysis revealed that the freezing point of the preservation solution was -1.4 °C (Fig. 7A). Subsequently, temperature changes were monitored in real time for the same solution placed in a cooling chamber maintained at -4 °C under magnetic flux densities of 0 mT, 5 mT, 10 mT, and 15 mT.

After reaching -4 °C, all samples were maintained at this temperature for a 30 min observation period. Under all magnetic field conditions, the solution samples remained unfrozen and maintained a stable supercooled state, as evidenced by the absence of visible ice formation and the absence of abrupt temperature increases associated with latent heat release. The temperature profiles exhibited nearly identical patterns regardless of the magnetic field intensity (Fig. 7B). As summarized in Table 2, all nine samples under each magnetic field condition successfully remained in the supercooled state throughout the observation period.

(Fig. 7)

(Table 2)

Effects of the Magnetic Field on Embryo Preservation

Embryo viability was evaluated after 24 hours of preservation under supercooled conditions at -4 °C. Fig. 8A shows the internal temperature of the cooling chamber during embryo preservation. In the temperature profile, oscillations were observed in the thermocouple readings due to magnetic field interference; however, these fluctuations did not affect the actual internal temperature, and the chamber temperature remained stable around -4 °C throughout the experimental period. Fig. 8B presents representative images of embryos observed after post-preservation culturing. The embryos were classified as survived, degenerated, or hatched based on their morphology. Table 3 summarizes the average survival rates of embryos preserved under different magnetic flux densities. The control group (0 mT) showed a mean survival rate of $48.66\% \pm 7.07\%$, while slightly higher survival rates were observed at 5 mT ($60.07\% \pm 5.48\%$) and 10 mT ($62.85\% \pm 5.24\%$), although these differences were not statistically significant. In contrast, the 15 mT

242 group exhibited the highest survival rate ($75.69\% \pm 4.31\%$), whereas the 20 mT group showed a slightly lower rate
243 ($68.96\% \pm 7.62\%$). Both the 15 mT and 20 mT groups demonstrated statistically significant differences compared
244 with the control samples ($p < 0.05$).

245 **(Fig. 8)**

246 **(Table 3)**

247

248 **Discussion**

249 Previous studies have demonstrated that commonly used hypothermic (2-8 °C) and cryopreservation (-196 °C)
250 approaches still have inherent limitations. In particular, these preservation methods cannot fully prevent cellular injury
251 caused by ice crystal formation, osmotic stress, and cryoprotectant toxicity [21]. Supercooling has emerged as a
252 promising alternative for short- and medium-term preservation, with accumulating evidence supporting its
253 applicability in agricultural and biological materials [22,23]. In this study, we applied supercooling preservation
254 combined with an oscillating magnetic field (OMF) to maintain the embryos at -4°C without ice formation.

255 As shown in Fig. 1 and Fig. 2, the Helmholtz-type dual-coil configuration and the double-jacket cooling chamber
256 were designed to minimize coil-induced heating, a factor known to destabilize supercooling environments [24]. Spatial
257 temperature measurements confirmed that the vertical and horizontal variations remained within ± 0.5 °C and ± 0.2 °C,
258 respectively (Fig. 5, Table 1), indicating that localized warming—which can trigger ice nucleation—was effectively
259 suppressed. Magnetic field measurements also showed high agreement with the simulation results, with discrepancies
260 within $\pm 5\%$ (Fig. 6), demonstrating that the preservation region received a uniform amount of magnetic flux.
261 Consequently, it was confirmed that the system provided a stable thermal and magnetic environment for evaluating
262 OMF effects.

263 Before conducting the embryo experiments, we examined whether different magnetic flux densities influenced the
264 cooling behavior of the preservation solution at -4 °C. Although magnetic field exposure was expected to stabilize
265 the supercooled state, Fig. 7 shows that the cooling curves were nearly identical across all groups, indicating no
266 measurable effect of the magnetic flux density on the cooling process. Consistent with these results, all samples
267 remained successfully supercooled regardless of the field intensity level (Table 2). These findings suggest that
268 thermodynamic parameters—such as the cooling rate, container geometry, solution composition, and sample
269 volume—play a more dominant role in determining supercooling stability than the magnetic field intensity under the
270 present conditions [19,25,26]. Importantly, the OMF did not induce premature nucleation, contrary to previous reports
271 proposing that an OMF can trigger ice formation [27]. Instead, our data indicates that the OMF posed minimal risk of
272 destabilizing the supercooled state within the tested intensity range. However, given that this study was conducted
273 under a limited range of magnetic field conditions, future studies are needed to investigate the interactions between
274 magnetic field parameters (intensity, frequency, waveform) and temperature on supercooling outcomes more
275 systematically [28].

276 Blastocyst-stage bovine embryos were preserved in the developed system at -4 °C for 24 hours and subsequently
277 cultured for 24 hours to assess viability. As shown in Table 3 and Fig. 8B, survival rates were higher in all magnetic
278 field groups compared with the control group (0 mT), with the highest viability observed at 15 mT (75.69%). The 15
279 mT group exhibited a statistically significant improvement relative to the controls ($p < 0.05$), whereas a slight decline

280 was observed at 20 mT. The temperature profile during preservation (Fig. 8A) confirmed that embryos experienced
281 stable -4°C conditions throughout the process, indicating that differences in survival were attributable to the magnetic
282 field intensity rather than to thermal fluctuations. Kojima et al. 2013 [29] reported that an appropriate combination of
283 the OMF intensity and freezing temperature can modulate intracellular ice formation and dehydration, thereby
284 improving post-thaw cell survival. This principle aligns with our results, in which viability increased under a specific
285 magnetic field condition. Similarly, studies using static magnetic fields (SMFs) have shown that SMFs can suppress
286 intracellular ice formation and oxidative stress, leading to improved cellular recovery after cryopreservation [30,31].
287 Although the present study applied an OMF under supercooling rather than freezing conditions, the peak survival
288 observed at 15 mT resembles the stabilizing effects reported for exposure to SMFs, raising the possibility that OMF-
289 induced stabilization effects could involve the modulation of ROS, membrane potential, or mitochondrial function.

290 In summary, this study demonstrated that exposure to an OMF at -4°C enhanced embryo survival. This finding
291 stands in contrast to previous reports showing that alternating magnetic fields can exert detrimental effects on
292 mammalian embryos—including increased ROS production, impaired cellular function, morphological abnormalities,
293 and reduced viability [32–34]. Embryo survival increased with the magnetic field intensity up to a certain threshold,
294 beyond which the enhancement plateaued, revealing a nonlinear response. This pattern suggests that a specific
295 magnetic field condition (e.g., 15 mT) may mitigate ROS accumulation or support the maintenance of DNA integrity
296 under low-temperature stress [35]. It is also conceivable that magnetic-field-assisted supercooling influenced the
297 physical state of the intracellular water or the local microenvironment [36]. Meanwhile, magnetic field intensities
298 below 10 mT or above 20 mT showed less pronounced improvements in embryo survival compared to the intermediate
299 field strength settings. Although the observed response may reflect the combined effects of the applied magnetic field
300 parameters, the potential influence of unequal sample sizes and batch-related variability across experimental groups
301 cannot be excluded. Accordingly, these factors should be more rigorously controlled in future studies.

302 The results of this study demonstrate the feasibility of OMF-assisted supercooling for embryo preservation,
303 indicating that magnetic fields may simultaneously stabilize the supercooled state and support the physiological
304 viability of embryos. However, this study has several limitations. First, only short-term post-preservation viability (1
305 day) was evaluated; therefore, future studies should assess long-term developmental outcomes (≥ 3 days), including
306 hatching and pregnancy rates. Second, the experiments were conducted under fixed temperature and frequency
307 conditions with a narrow range of magnetic field intensity levels, implying that further research should systematically
308 examine the interactions among temperature conditions and magnetic field parameters (waveform, intensity,
309 frequency). Finally, while several potential biological mechanisms may be hypothesized to explain the observed
310 effects of OMF exposure, these were not directly examined in the present study. Therefore, future studies should
311 directly assess molecular and cellular indicators—such as ROS levels, the membrane potential, Ca^{2+} dynamics, and
312 the mitochondrial membrane potential ($\Delta\Psi\text{m}$)—to validate these hypotheses.

313

314 Conclusion

315 In this study, we developed and evaluated an OMF-assisted supercooling system for the preservation of bovine IVF
316 embryos at -4°C . The combined use of Helmholtz coils and a circulation-based cooling system ensured uniform
317 thermal and magnetic field stability, and no freezing occurred under any condition. Embryo survival was significantly

318 improved at 15 mT compared with the control group, indicating that magnetic fields may enhance cellular stability
319 within a specific intensity range during supercooling preservation.

320 In contrast, no thermodynamic differences were detected in the preservation solution, suggesting that factors such
321 as the cooling rate and container geometry exert stronger control over supercooling behavior than magnetic field
322 exposure. Future studies should quantitatively assess the interactions among magnetic field parameters and
323 temperature conditions and further evaluate long-term developmental outcomes, including hatching and pregnancy
324 rates.

325 Collectively, these findings demonstrate that an OMF can simultaneously suppress freezing and improve embryo
326 survival during supercooling, providing a foundational basis for magnetic-field-based, non-freezing preservation
327 strategies for biological specimens.

328

ACCEPTED

329 **References**

330 1. Sirard M-A. 40 years of bovine IVF in the new genomic selection context. *Reproduction*. Bioscientifica Ltd;
331 2018;156:R1–7. <https://doi.org/10.1530/REP-18-0008>

332 2. Huang Z, Gao L, Hou Y, Zhu S, Fu X. Cryopreservation of farm animal gametes and embryos: recent updates and
333 progress. *Front Agr Sci Eng*. 2019;6:42–53. <https://doi.org/10.15302/J-FASE-2018231>

334 3. Valente RS, Marsico TV, Sudano MJ. Basic and applied features in the cryopreservation progress of bovine
335 embryos. *Animal Reproduction Science*. 2022;239:106970. <https://doi.org/10.1016/j.anireprosci.2022.106970>

336 4. Marqui FN, Martins A, Cardoso TC, Cruz TE, Dell'Aqua JA, Oba E. Cooling of in vitro-produced bovine
337 embryos: Effects of medium and time on gene expression, DNA fragmentation and embryonic survival. *Livestock
338 Science*. 2019;230:103811. <https://doi.org/10.1016/j.livsci.2019.09.027>

339 5. Fuller BJ, Petrenko AY, Rodriguez JV, Somov AY, Balaban CL, Guibert EE. Biopreservation of Hepatocytes:
340 Current Concepts on Hypothermic Preservation, Cryopreservation, And Vitrification. *Cryoletters*. 2013;37:432–52.

341 6. I detta A, Aoyagi Y, Tsuchiya K, Kamijima T, Nishimiya Y, Tsuda S. A simple medium enables bovine embryos
342 to be held for seven days at 4°C. *Sci Rep*. Nature Publishing Group; 2013;3:1173. <https://doi.org/10.1038/srep01173>

343 7. I detta A, Aoyagi Y, Tsuchiya K, Nakamura Y, Hayama K, Shirasawa A, et al. Prolonging hypothermic storage (4
344 C) of bovine embryos with fish antifreeze protein. *J Reprod Dev*. 2015;61:1–6. <https://doi.org/10.1262/jrd.2014-073>

345 8. Murray KA, Gao Y, Griffiths CA, Kinney NLH, Guo Q, Gibson MI, et al. Chemically Induced Extracellular Ice
346 Nucleation Reduces Intracellular Ice Formation Enabling 2D and 3D Cellular Cryopreservation. *JACS Au*.
347 American Chemical Society; 2023;3:1314–20. <https://doi.org/10.1021/jacsau.3c00056>

348 9. Preciado J, Rubinsky B. The effect of isochoric freezing on mammalian cells in an extracellular phosphate
349 buffered solution. *Cryobiology*. 2018;82:155–8. <https://doi.org/10.1016/j.cryobiol.2018.04.004>

350 10. Usta OB, Kim YH, Ozer S, Bruinsma BG, Lee JW, Demir E, et al. Supercooling as a Viable Non-Freezing Cell
351 Preservation Method of Rat Hepatocytes. *PLoS One*. 2013;8:e69334. <https://doi.org/10.1371/journal.pone.0069334>

352 11. William N, Isiksacan Z, Mykhailova O, Olafson C, Yarmush ML, Usta OB, et al. Comparing two extracellular
353 additives to facilitate extended storage of red blood cells in a supercooled state. *Frontiers in Physiology [Internet]*.
354 2023 [cited 2024 Jan 16];14. <https://www.frontiersin.org/articles/10.3389/fphys.2023.1165330>. Accessed 16 Jan
355 2024

356 12. Hikichi M, Shimizu T, Sato K. Development of supercooling preservation method of adherent cultured human
357 cells. *The Journal of Biochemistry*. 2023;174:273–8. <https://doi.org/10.1093/jb/mvad040>

358 13. Huang H, Yarmush ML, Usta OB. Long-term deep-supercooling of large-volume water and red cell suspensions
359 via surface sealing with immiscible liquids. *Nat Commun*. Nature Publishing Group; 2018;9:3201.
360 <https://doi.org/10.1038/s41467-018-05636-0>

361 14. Gholami D, Ghaffari SM, Riazi G, Fathi R, Benson J, Shahverdi A, et al. Electromagnetic field in human sperm
362 cryopreservation improves fertilizing potential of thawed sperm through physicochemical modification of water
363 molecules in freezing medium. *PLOS ONE*. Public Library of Science; 2019;14:e0221976.
364 <https://doi.org/10.1371/journal.pone.0221976>

365 15. Gou Y, Qin Y, Li J, Zhang W, Liu J, Wang Z. Effect of a magnetic field on droplet freezing and frost formation
366 on cold surfaces. *Cryobiology*. 2024;114:104866. <https://doi.org/10.1016/j.cryobiol.2024.104866>

367 16. Jun S, Ko YB, Lee SH. Explorative Supercooling Technology for Prevention of Freeze Damages in Vaccines.
368 Applied Sciences. Multidisciplinary Digital Publishing Institute; 2022;12:3173.
369 <https://doi.org/10.3390/app12063173>

370 17. Kong F, Li P, Zhang H, Tian C, Leng D, Hou C. Enhanced Supercooling of Water with a 6 mT/50 Hz
371 Oscillating Magnetic Field and its Application in Fruit Preservation. *Food Bioprocess Technol* [Internet]. 2024
372 [cited 2024 May 24]; <https://doi.org/10.1007/s11947-024-03384-2>

373 18. Ju BH, Kim YJ, Park YB, Kim BH, Kim MK. Evaluation of conical 9 well dish on bovine oocyte maturation and
374 subsequent embryonic development. *Journal of Animal Science and Technology*. Korean Society of Animal Science
375 and Technology; 2024;66:936–48. <https://doi.org/10.5187/jast.2024.e68>

376 19. Kang TY, Hoptowit R, Jun SJ. Effects of an oscillating magnetic field on ice nucleation in aqueous iron-oxide
377 nanoparticle dispersions during supercooling and preservation of beef as a food application. *Journal of Food Process
378 Engineering*. 2020;43:e13525. <https://doi.org/10.1111/jfpe.13525>

379 20. Beguš S, Bojkovski J, Drnovšek J, Geršak G. Magnetic effects on thermocouples. *Meas Sci Technol*. IOP
380 Publishing; 2014;25:035006. <https://doi.org/10.1088/0957-0233/25/3/035006>

381 21. Elliott GD, Wang S, Fuller BJ. Cryoprotectants: A review of the actions and applications of cryoprotective
382 solutes that modulate cell recovery from ultra-low temperatures. *Cryobiology*. 2017;76:74–91.
383 <https://doi.org/10.1016/j.cryobiol.2017.04.004>

384 22. Jiang H, Hong W, Zhang Y, Liu S, Jiang H, Xia S, et al. Effects of static magnetic field-prolonged supercooling
385 preservation on blueberry quality. *Food Bioscience*. 2024;59:103771. <https://doi.org/10.1016/j.fbio.2024.103771>

386 23. Lee DY, You YS, Ho KKHY, Li Y, Jun SJ. Impact of supercooling storage on physical and chemical properties
387 of yellowfin tuna (*Thunnus albacares*). *Journal of Food Engineering*. 2024;373:111818.
388 <https://doi.org/10.1016/j.jfoodeng.2023.111818>

389 24. Kang TY, You YS, Hoptowit R, Wall MM, Jun SJ. Effect of an oscillating magnetic field on the inhibition of ice
390 nucleation and its application for supercooling preservation of fresh-cut mango slices. *Journal of Food Engineering*.
391 2021;300:110541. <https://doi.org/10.1016/j.jfoodeng.2021.110541>

392 25. Otero L, Rodríguez AC, Pérez-Mateos M, Sanz PD. Effects of Magnetic Fields on Freezing: Application to
393 Biological Products. *Comprehensive Reviews in Food Science and Food Safety*. 2016;15:646–67.
394 <https://doi.org/10.1111/1541-4337.12202>

395 26. John Morris G, Acton E. Controlled ice nucleation in cryopreservation – A review. *Cryobiology*. 2013;66:85–92.
396 <https://doi.org/10.1016/j.cryobiol.2012.11.007>

397 27. Ruan J, Wang H, Zhao J, Li D, Yang H. Effect of Magnetic Field on Frozen Food Quality Characteristics. *Food
398 Eng Rev*. 2024;16:396–421. <https://doi.org/10.1007/s12393-024-09366-6>

399 28. Rodríguez AC, Otero L, Cobos JA, Sanz PD. Electromagnetic Freezing in a Widespread Frequency Range of
400 Alternating Magnetic Fields. *Food Eng Rev*. 2019;11:93–103. <https://doi.org/10.1007/s12393-019-09190-3>

401 29. Kojima S, Kaku M, Kawata T, Sumi H, Shikata H, Abonti TR, et al. Cryopreservation of rat MSCs by use of a
402 programmed freezer with magnetic field. *Cryobiology*. 2013;67:258–63.
403 <https://doi.org/10.1016/j.cryobiol.2013.08.003>

404 30. Baniasadi F, Hajiaghalyou S, Shahverdi A, Ghalambor MR, Pirhajati V, Fathi R. The Beneficial Effects of
405 Static Magnetic Field and Iron Oxide Nanoparticles on the Vitrification of Mature Mice Oocytes. *Reprod Sci*.
406 2023;30:2122–36. <https://doi.org/10.1007/s43032-022-01144-1>

407 31. Baniasadi F, Hajiaghalyou S, Shahverdi A, Pirhajati V, Fathi R. Static magnetic field halves cryoinjuries of
408 vitrified mouse COCs, improves their functions and modulates pluripotency of derived blastocysts. *Theriogenology*.
409 2021;163:31–42. <https://doi.org/10.1016/j.theriogenology.2020.12.025>

410 32. Zadeh-Haghghi H, Simon C. Magnetic field effects in biology from the perspective of the radical pair
411 mechanism. *Journal of The Royal Society Interface*. Royal Society; 2022;19:20220325.
412 <https://doi.org/10.1098/rsif.2022.0325>

413 33. Chen JS, Tsai LK, Yeh TY, Li TS, Li CH, Wei ZH, et al. Effects of electromagnetic waves on oocyte maturation
414 and embryonic development in pigs. *J Reprod Dev.* 2021;67:392–401. <https://doi.org/10.1262/jrd.2021-074>

415 34. Seify M, Khalili MA, Anbari F, Koohestanidehaghi Y. Detrimental effects of electromagnetic radiation emitted
416 from cell phone on embryo morphokinetics and blastocyst viability in mice. *Zygote.* 2024;32:149–53.
417 <https://doi.org/10.1017/S0967199424000042>

418 35. Dahr NK, Abdolmaleki P, Halvaei I. Static magnetic field can ameliorate detrimental effects of cryopreservation
419 on human spermatozoa. *Rev Int Androl.* 2024;22:27–34. <https://doi.org/10.22514/j.androl.2024.012>

420 36. Okuda K, Kaori K, Kawauchi A, Miyu I, Yomogida K. An oscillating magnetic field suppresses ice-crystal
421 growth during rapid freezing of muscle tissue of mice. *The Journal of Biochemistry.* 2023;mvad087.
422 <https://doi.org/10.1093/jb/mvad087>

423

424

ACCEPTED

List of Tables

425

426 **Table 1. Temperature Distribution at Each Point within the Chamber**

427 **Table 2. Frequency of the Supercooled Preservation Solution**

428 **Table 3. Effects of the Magnetic Flux Density on the Survival Rate of Bovine Embryos during Supercooling**
429 **Preservation**

430

431 **Table 1. Temperature Distribution at Each Point within the Chamber**

Temperature point	Average (°C)	Min (°C)	Max (°C)
Top	0.05 (± 0.02)	-0.02	0.14
Middle		Ref	
Bottom	-0.04 (± 0.02)	-0.11	0.02
①		Ref	
②	-0.006 (± 0.018)	-0.08	0.06
③	0.006 (± 0.02)	-0.07	0.09
④	0.015 (± 0.023)	-0.07	0.10

432

433 **Table 2. Frequency of the Supercooled Preservation Solution**

Magnetic flux density (mT)	No. of sample	No. of Supercooled
0 (Control)	9	9
5	9	9
10	9	9
15	9	9

434

435 **Table 3. Effects of the Magnetic Flux Density on the Survival Rate of Bovine Embryos during Supercooling**
436 **Preservation**

Magnetic flux density (mT)	No. of Embryos	No. of Survived (%)
0 (Control)	31	15 (48.66 \pm 7.07) ^a
5	35	21 (60.07 \pm 5.48) ^a
10	35	21 (62.85 \pm 5.24) ^a
15	32	24 (75.69 \pm 4.31) ^b
20	28	19 (68.96 \pm 7.62) ^b

* Different letters indicate significant differences ($p < 0.05$).

437

438

ACCEPTED

439

List of Figures

440

Fig. 1. Design of the oscillating-magnetic-field (OMF)-assisted supercooling system: (A) Schematic diagram of the system. (B) Overall system assembly with a Helmholtz coil and a control unit. (C) Heat-dissipation structure showing heat sinks and the airflow design.

441

Fig. 2. Structure of the embryo preservation chamber: (A) Double-wall acrylic chamber with a three-tier rack holding twelve sample tubes (four per layer). (B) Cooling mechanism showing the flow of propylene-glycol coolant between the inner and outer walls.

442

Fig. 3. Geometry of the Helmholtz coil: (A) Design drawing of the Helmholtz coil showing two identical circular coils arranged with a spacing equal to the coil radius. (B) 3D simulation geometry constructed in COMSOL Multiphysics, representing the model used for the magnetic field calculation. The coordinate axes are expressed in millimeters (mm).

443

Fig. 4. Experimental workflow of the oscillating-magnetic-field-assisted supercooling procedure for bovine embryos. The process consists of three main stages: (1) *Preparation* — a single IVF-derived bovine blastocyst was placed in a 1.2 mL tube containing a preservation solution; (2) *Preservation* — samples were stored at -4°C under oscillating magnetic fields (0-20 mT) for 23 h, followed by 1 h of warming at 4°C ; (3) *Post-preservation evaluation* — embryos were incubated at 38.5°C for 24 h, and viability was assessed based on survival and apoptosis outcomes.

444

Fig. 5. Temperature measurement point inside the cooling chamber: (A) Vertical and (B) Horizontal.

445

Fig. 6. Magnetic flux density distribution of the Helmholtz coil: (A) simulated magnetic field lines of the Helmholtz configuration, (B) oscillating magnetic field generated by a bipolar pulse voltage, (C) axial magnetic flux distribution obtained from the simulation, and (D) comparison between simulated and experimentally measured magnetic flux densities along the y-axis, showing that both results agree within $\pm 5\%$ around the target field strength (15 mT).

446

Fig. 7. Cooling behavior of the preservation solution under oscillating magnetic field conditions: (A) The DSC analysis revealed a freezing point at -1.4°C . (B) The temperature profiles obtained under a magnetic field intensity range of 0-15 mT exhibited nearly identical cooling curves.

447

Fig. 8. Embryo supercooling preservation results: (A) Temperature profile within the chamber under OMF and non-OMF conditions during embryo preservation. (B) Microscopic image showing the typical morphology of embryos surviving and degenerating after supercooling preservation

448

449

450

451

452

453

454

455

456

457

458

459

460

461

462

463

464

465

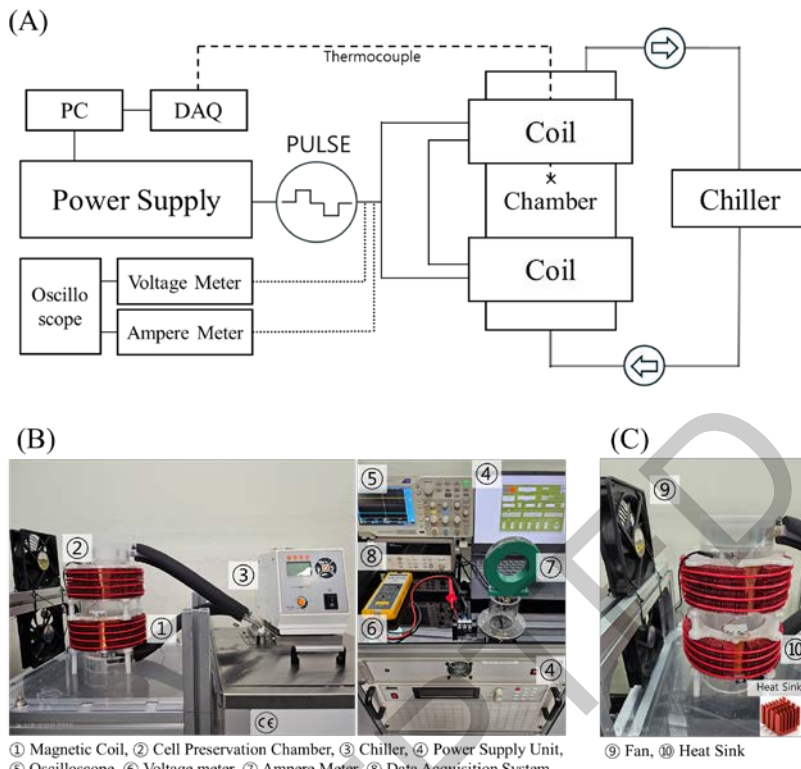
466

467

468

468
469
470

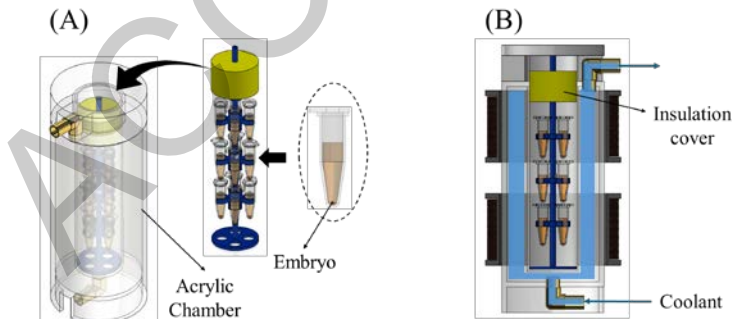
Fig. 1. Design of the oscillating-magnetic-field (OMF)-assisted supercooling system: (A) Schematic diagram of the system. (B) Overall system assembly with a Helmholtz coil and a control unit. (C) Heat-dissipation structure showing heat sinks and the airflow design



471

472
473
474
475

Fig. 2. Structure of the embryo preservation chamber: (A) Double-wall acrylic chamber with a three-tier rack holding twelve sample tubes (four per layer). (B) Cooling mechanism showing the flow of propylene-glycol coolant between the inner and outer walls.

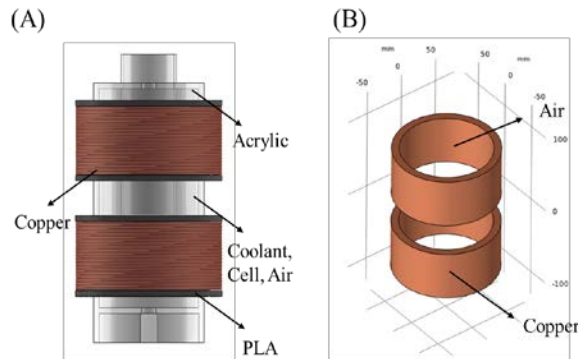


476

477

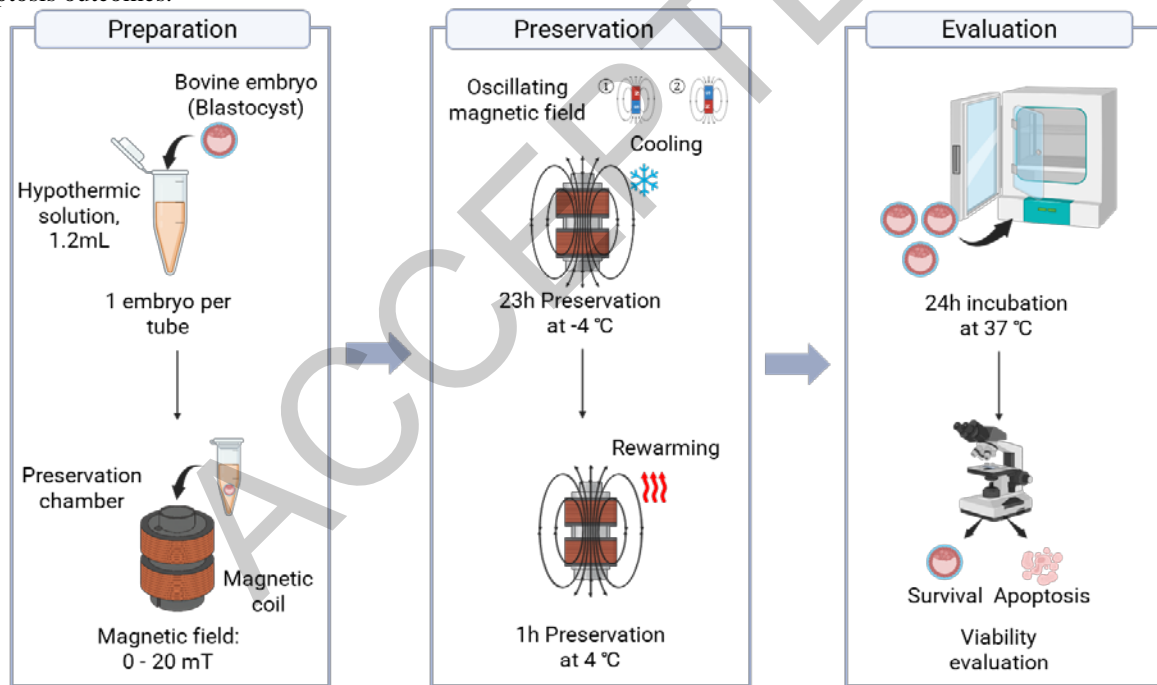
478
479
480
481

Fig. 3. Geometry of the Helmholtz coil. (A) Design drawing of the Helmholtz coil showing two identical circular coils arranged with a spacing equal to the coil radius. (B) 3D simulation geometry constructed in COMSOL Multiphysics, representing the model used for the magnetic field calculation. The coordinate axes are expressed in millimeters (mm).



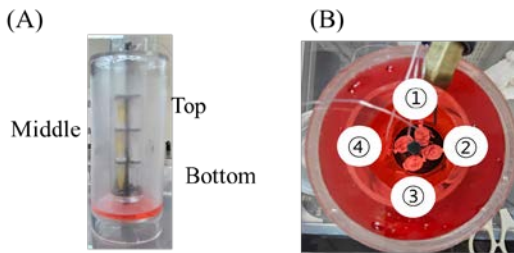
482
483
484
485
486
487
488
489

Fig. 4. Experimental workflow of the oscillating-magnetic-field-assisted supercooling procedure for bovine embryos. The process consists of three main stages: (1) Preparation — a single IVF-derived bovine blastocyst was placed in a 1.2 mL tube containing a preservation solution; (2) Preservation — samples were stored at -4°C under oscillating magnetic fields (0-20 mT) for 23 h, followed by 1 h of warming at 4°C ; (3) Post-preservation evaluation — embryos were incubated at 38.5°C for 24 h, and viability was assessed based on survival and apoptosis outcomes.



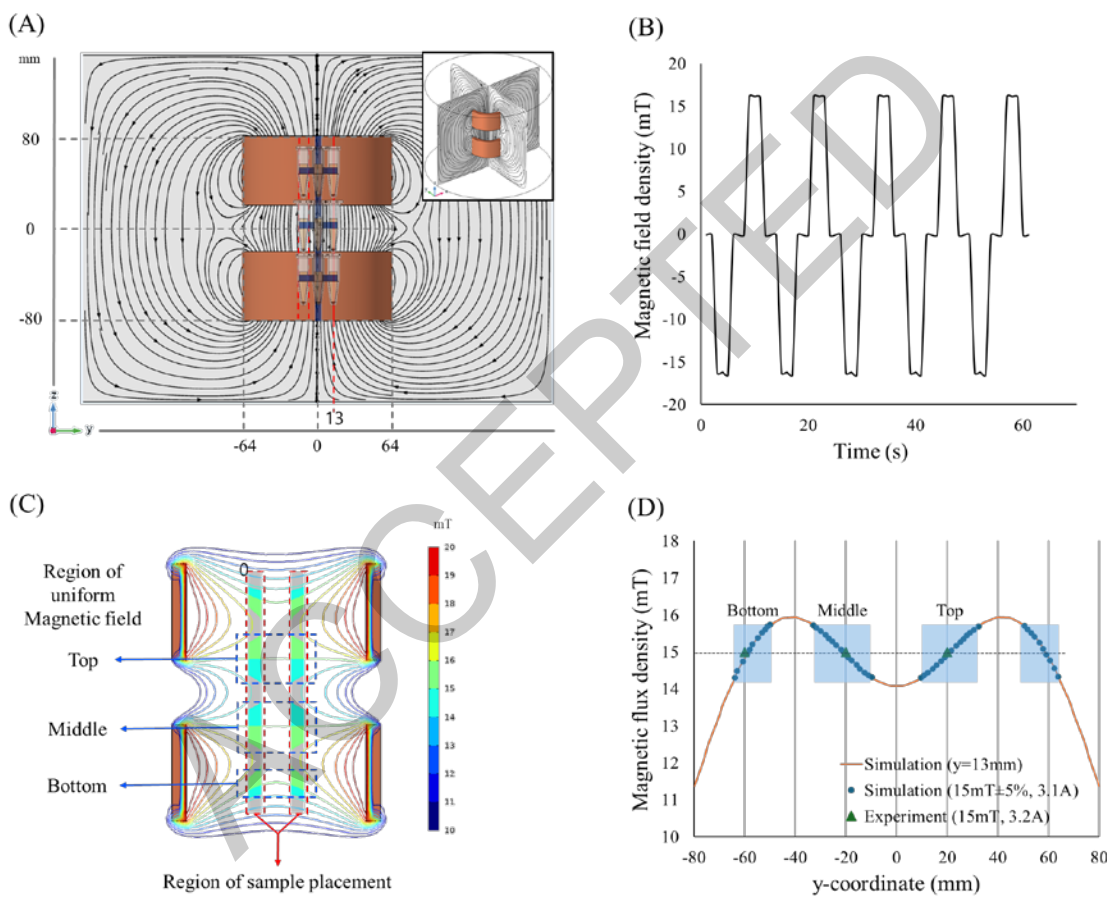
490
491

492 **Fig. 5. Temperature measurement point inside the cooling chamber:** (A) Vertical and (B) Horizontal.



493
494

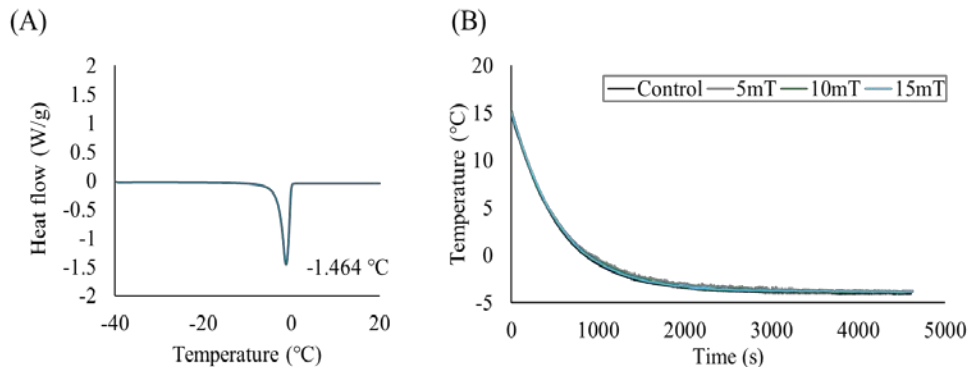
495 **Fig. 6. Magnetic flux density distribution of the Helmholtz coil:** (A) simulated magnetic field lines of the Helmholtz
496 configuration, (B) oscillating magnetic field generated by a bipolar pulse voltage, (C) axial magnetic flux distribution
497 obtained from the simulation, and (D) comparison between simulated and experimentally measured magnetic flux
498 densities along the y-axis, showing that both results agree within $\pm 5\%$ around the target field strength (15 mT).



499

500

501 **Fig. 7. Cooling behavior of the preservation solution under oscillating magnetic field conditions:** (A) The DSC
 502 analysis revealed a freezing point at -1.4°C . (B) The temperature profiles obtained under a magnetic field intensity
 503 range of 0-15 mT exhibited nearly identical cooling curves.



504
 505
 506 **Fig. 8. Embryo supercooling preservation results:** (A) Temperature profile within the chamber under OMF and
 507 non-OMF conditions during embryo preservation. (B) Microscopic image showing the typical morphology of
 508 embryos surviving and degenerating after supercooling preservation

